Supplementary Information

Contents

Biotinylated vesicles and coating efficiency

Liposomes with a high degree of biotinylation (0.02%), considered more complex than POPC:POPG liposomes due to hydrophobic biotin moieties, show increased stiction and finally irreversible adsorption on the lipid coated channel walls. In Figure S2a, biotinylated liposomes were trapped in a nanofluidics device coated with phospholipds (POPC:POPG 3:1). After 30 minutes, the channels are washed with clean buffer and imaged. The DiO

signal in Figure S2a shows the irreversible adsorption of the biotinylated vesicles on the nanochannel walls. Other attempts to patch the lipid coating with proteins and surfactants at low concentration, under the assumption that the stiction was due to an incomplete phospholipid coating, were unsuccessful. Specifically, Bovine Serum Albumin (BSA, 30 nM in 1xPBS) was flushed through the micro- and nanochannels after the phospholipid coating. The hypothesis is that the nanometer-sized protein would 'patch' the coating up. However, bright spots on the average intensity images show that vesicle stiction takes place (Figure S2b). Stiction is evident from the bright spots after averaging the movies which indicates non-diffusing liposomes. Another attempt to improve the lipid coating efficiency is to incorporate a low percentage of surfactant (here Pluronic F-127 at low concentration 10^{-6} % w/v) in the liposome solution. The hypothesis is that the surfactant could decrease the interactions between vesicles or vesicles and the coating. However, stiction on the lipid coating was observed with the biotinylated liposomes (Figure S2c). Finally, a Pluronic F127 (1% w/v) coating was implemented which presents successful inhibition of vesicle adsorption or stiction.

Osmotic flow calibration in Device 1 and Device 2.

The osmotic flow calibration experiment quantifies the diffusioosmotic mobility and effective zeta potential of our low-potential coatings while identifying parasitic flows within the channel.[18,35]

We employ Streptavidin fluorescently labeled with Alexa Fluor 568 (SA-A568) from Thermo Fisher Scientific (catalog number S11226) as a neutral tracer unaffected by diffusiophoresis. The protein has a molecular weight of 52 kDa and a diffusion coefficient $D_{SA} = 70$ µm^2/s. In steady state, the dye concentration $\rho(x)$ in the nanochannel satisfies:

$$-D_{SA} h w(x) \partial_x \rho(x) + Q\rho(x) = \text{constant} \tag{1}$$

With boundary conditions $\rho(0) = \rho_L$ and $\rho(L) = \rho_H$, the solution takes the form:

$$\rho(x) = q_1 + q_2 w(x)^\alpha \tag{2}$$

$$\text{where } \alpha = \frac{Q}{Dh\Delta w/L},\ q_1 = \frac{\rho_L w_H^\alpha - \rho_H w_L^\alpha}{w_H^\alpha - w_L^\alpha},\ q_2 = \frac{\rho_H - \rho_L}{w_H^\alpha - w_L^\alpha} \tag{3}$$

For our funnel-shaped nanochannel, the osmotic flow is expressed as:

$$Q = \frac{h}{L}\left[\frac{\Delta w}{\ln\left(1 + \frac{\Delta w}{w_L}\right)}\right]\Gamma_{os} \cdot \ln(\frac{c_L}{c_H}) + Q_{par} \tag{4}$$

The diffusioosmotic mobility Γ_{os} relates to the coating's zeta potential ζ_{ch} through eq.(5):

$$\Gamma_{os} = -\frac{\epsilon}{\eta}\frac{k_B T}{Ze}\left[\beta\zeta_{ch} - 2\frac{k_B T}{Ze}\ln\left(1 - \tanh^2\left(\frac{Ze}{4k_B T}\zeta_{ch}\right)\right)\right] \tag{5}$$

By measuring the fluorescence intensity profiles at various concentration gradients, we can determine the coating's zeta potential by fitting the experimental data to these equations. We also extract the flow rate with no gradient $Q_{par} = Q(\ln(\frac{c_L}{c_H}) = 0)$, which is a chip-related parameter measuring the residual flow rate. The residual flow rate is the result of Poisseuille flow induced in the nanochannels by pressure driven flows in the microchannels and the tolerance of the pressures applied to the device inlets combined. Results, shown in Figure S6, display a residual flow rate of -28 fL/min for Design 1 (L = 440 µm).

Liposome purification in protein background in a short trap.

We successfully trap liposomes in a 250 µm nanochannel length with a strong gradient as shown in Figure S7. We then introduce BSA at 1 µM for 15 minutes and finally we introduce clean buffers to separate the particles from the proteins. We hypothesize that the protein is temporarily deposited on the channel walls and then is able to be removed. We expect

this due to Pluronic ability to decrease protein adsorption on the nanochannel walls. We fit the particle distribution with our model for parameters of the channel zeta potential. The zeta potential of the coating becomes less negative when protein is diffusing in the nanochannel and the values are approximately equal before protein introduction and after protein removal.

Supplementary Figures

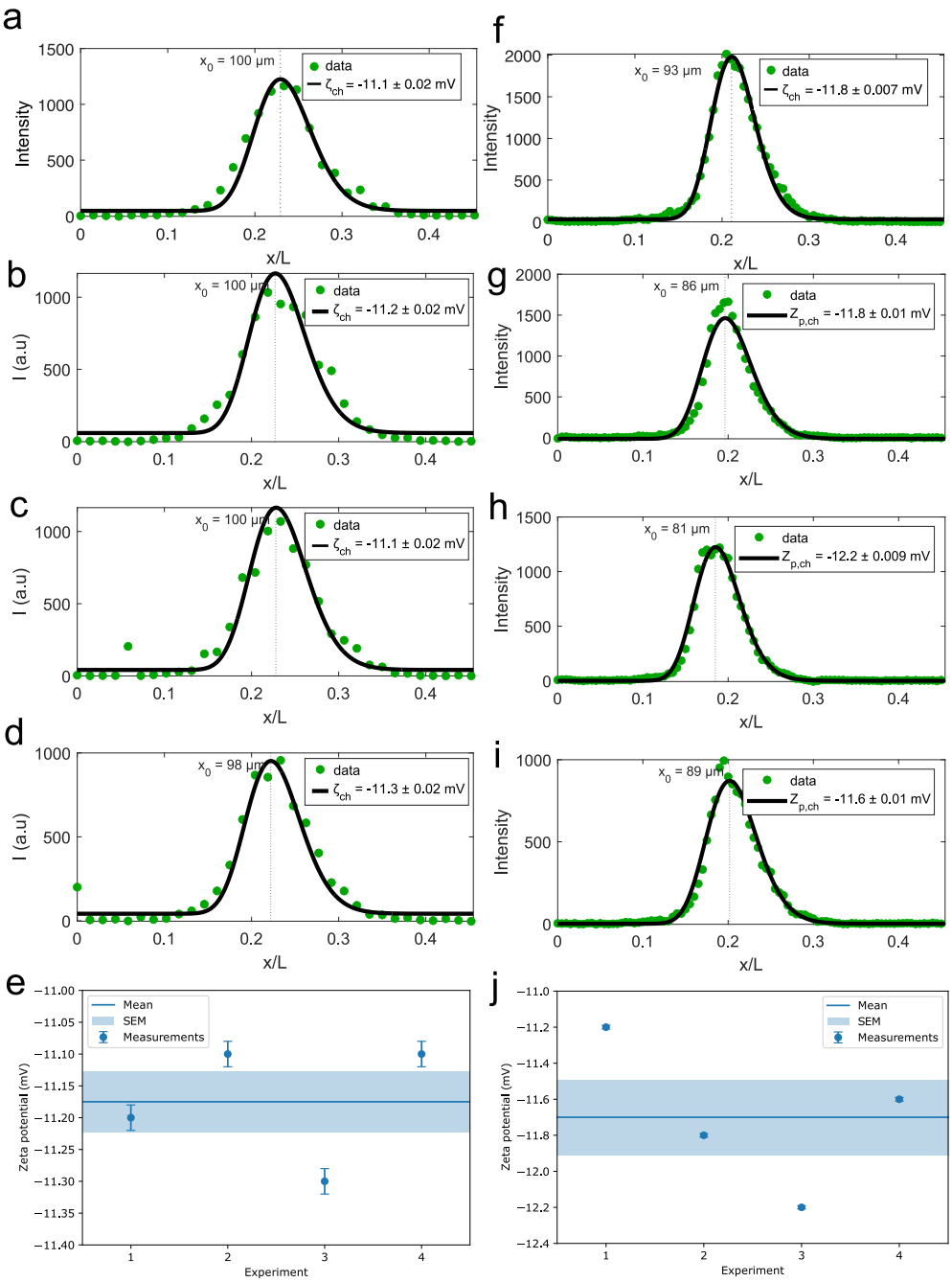

Fig. S1: **Fits of the wall zeta potential.** Liposome DiO signal (green) and fit (black) for four nanochannels in the experiment leading to the wall zeta potential using liposomes (a-d) and biotinylated liposomes (f-i). Data shown in a and f are identical to the main figure 1 panel h and i respectively. (e) The mean and s.e.m is -11.17 ± 0.05 mV. (j) The mean and s.e.m is -11.70 ± 0.21 mV.

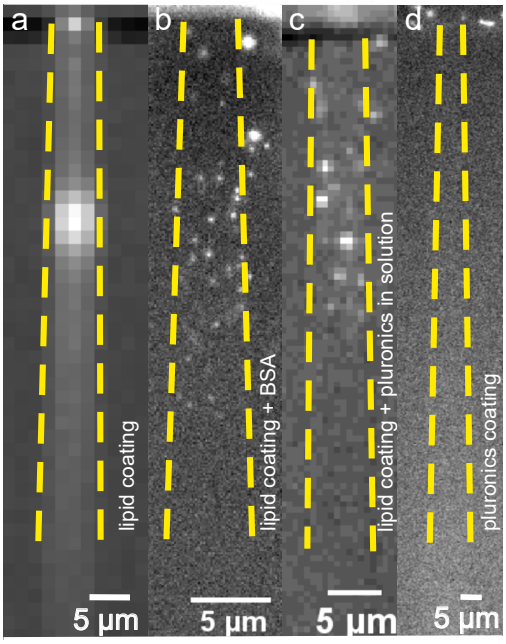

Fig. S2: **Fluorescence images of nanochannels after trapping of biotinylated liposomes.** DiO signal recorded after trapping of biotinylated liposomes and washing with clean buffer for channels coated with (a) lipid coating (POPC:POPG 3:1), (b) lipid coating and BSA (30 nM), (c) lipid coating and Pluronic F-127 (10^{-6}%) in solution, and (d) Pluronic F-127 (1% w/v) coating. The Pluronic coating inhibits vesicle adsorption or fusion with the nanochannel walls. Fluorescence images are recorded at different magnifications, scale bar is 5 µm.

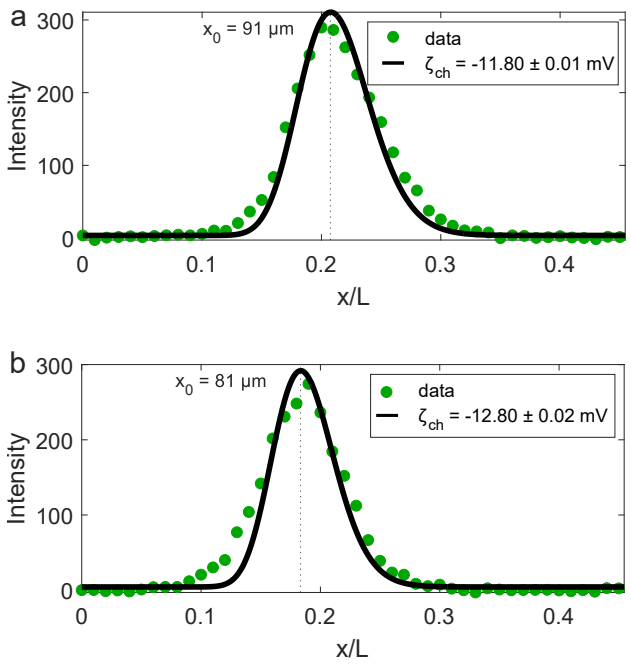

Fig. S3: **Successful liposome purification from a BSA micromolar background.** (a) Fluorescence intensity profile and fit of the channel zeta potential ζ_{ch} before BSA introduction (data Figure 2a red), and (b) after removal of BSA (data Figure 2a green).

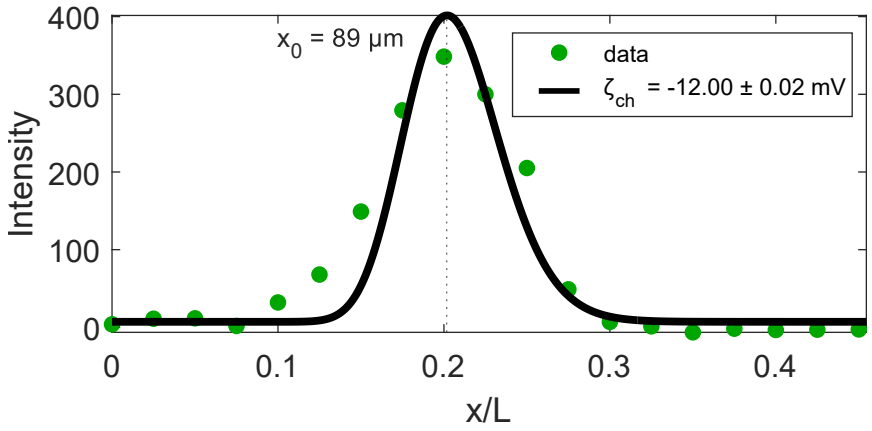

Fig. S4: **Characterization of the channel zeta potential ζ_{ch} after removal of the HSA micromolar background**. Fluorescence intensity profile of the liposomes after HSA removal (Figure 2e yellow curve) and fit to the channel zeta potential ζ_{ch}.

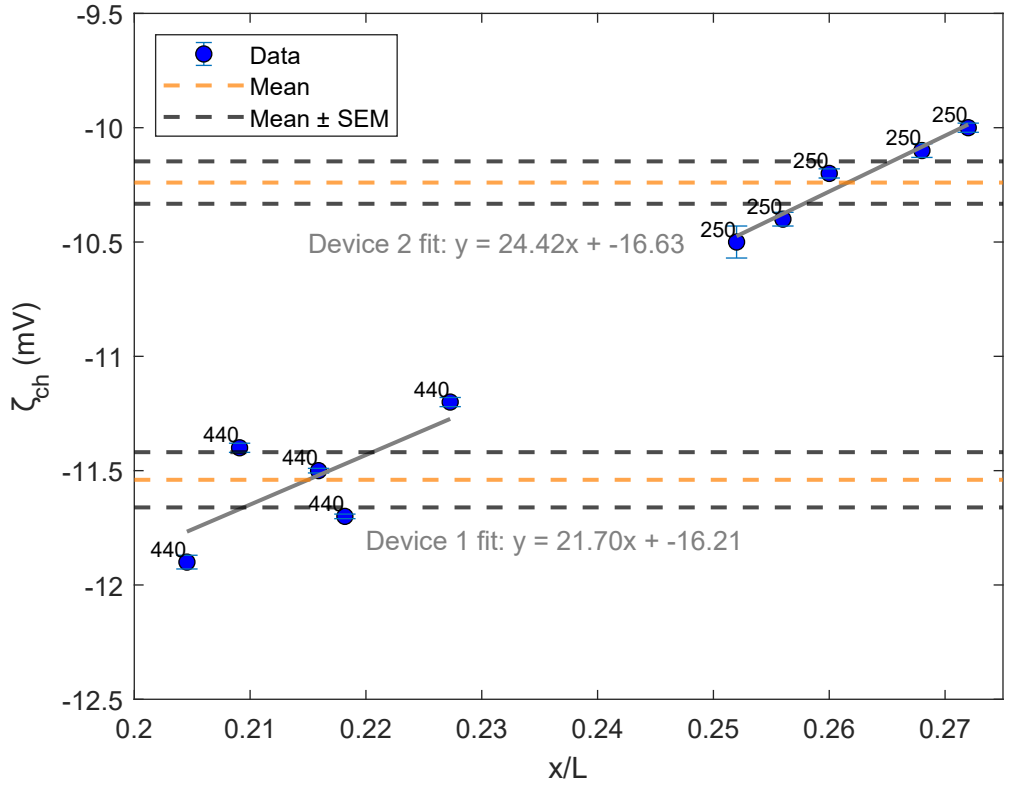

Fig. S5: **Comparison of ζ_{ch} obtained for short and long nanochannel designs.** The ζ_{ch} obtained from a fit to a well-characterized liposome distribution is plotted against the trapping position, x_0/L, and the mean and standard error of the mean, along with a linear fit for the two nanochannel lengths shows grouping dependent on the device design (Device design 1 or Device design 2).

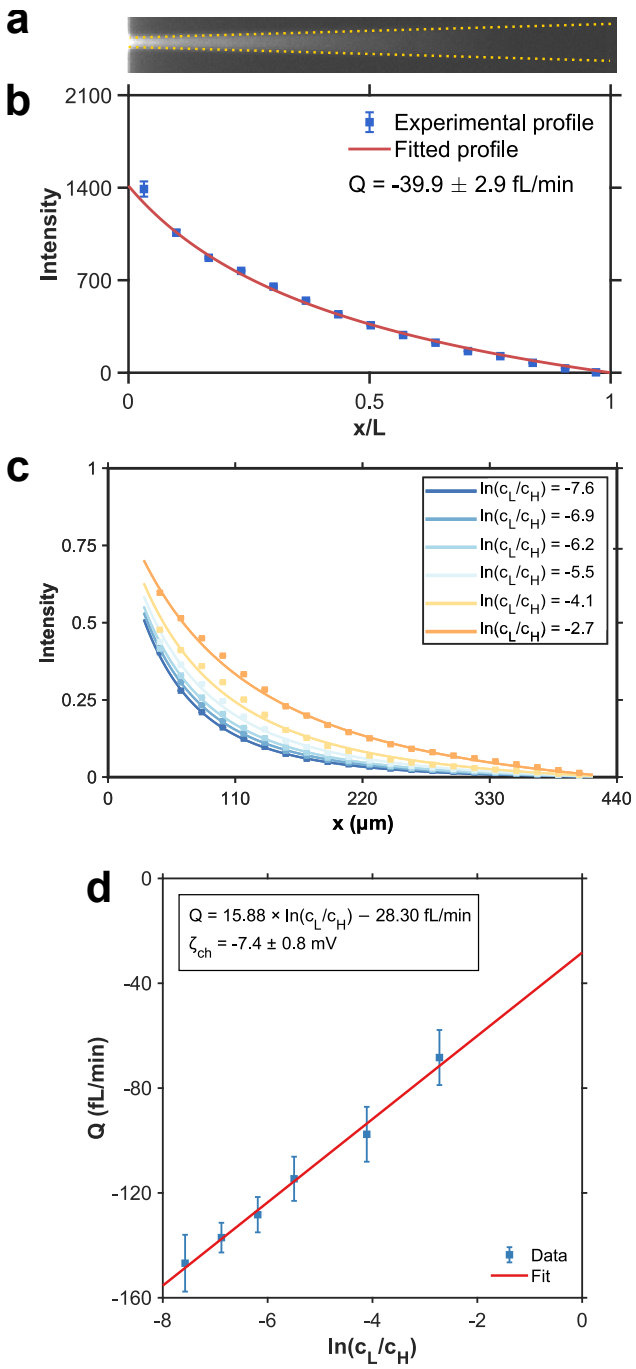

Fig. S6: **Osmotic and residual flow calibration of the Device 1 (L= 440 µm).** **(a)** Fluorescence microscopy image of a L=440 µm nanochannel under a salt gradient of $\ln(c_L/c_H) = -6.2$. **(b)** Corresponding intensity profile along the channel. **(c)** Normalized intensity profiles under various salt gradients for POPC:POPG 19:1. **(d)** Flow rate as a function of the salt gradient for the 19:1 coating, including a linear fit and the extracted zeta potential and residual flow rate.

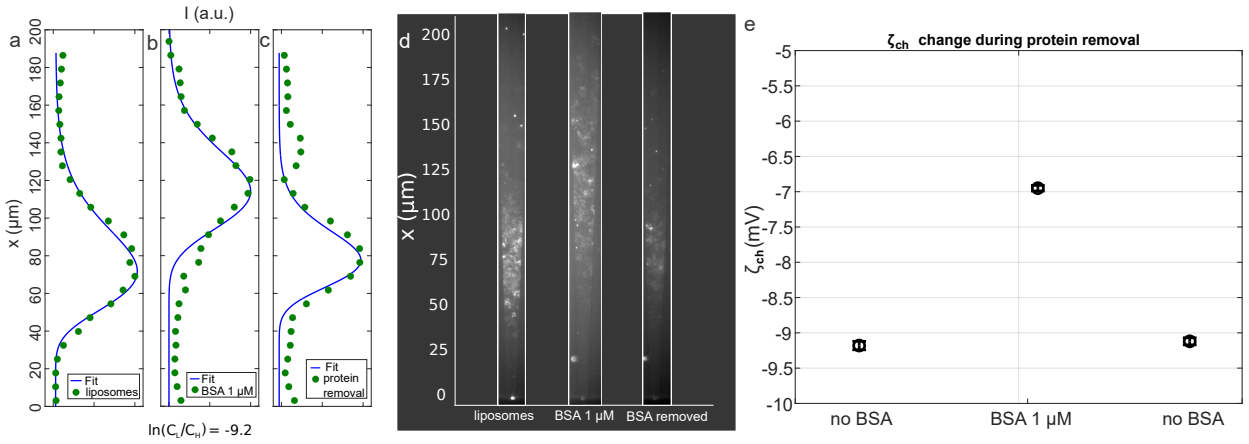

Fig. S7: **Change in trapping position due to the diffusioosmotic flow contribution of the protein gradient.** The distribution of well-characterized particles is fitted for the channel zeta potential in Device 2. (a) Trapped liposomes in a strong gradient with ζ_{ch} = -9.18 ± 0.06 mV at $x_0 = 72\,\mu m$, (b) while introducing BSA at 1 µM with $\zeta_{ch} = -6.95 \pm 0.04$ mV at $x_0 = 114\,\mu m$ for 15 minutes, and (c) after protein separation with $\zeta_{ch} = -9.12 \pm 0.05$ mV at $x_0 = 78\,\mu m$. (d) Fluorescence images (DiO) of the particle distribution. (e-f) Diameter and zeta potential of the coating changes during protein introduction and separation.

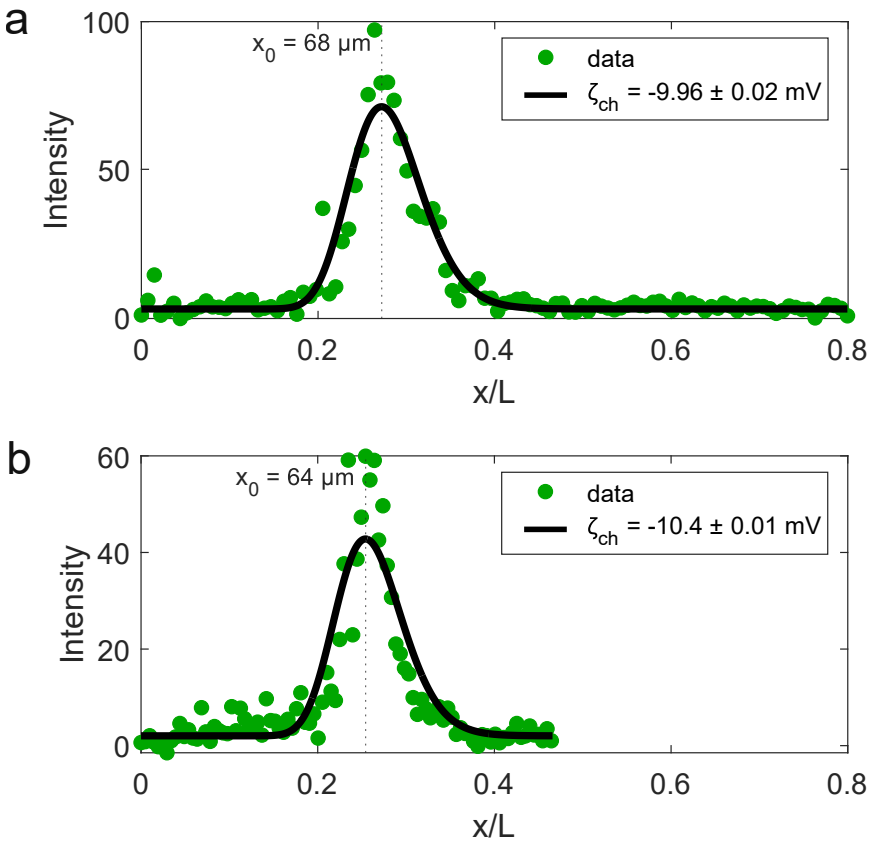

Fig. S8: **Characterization of the channel zeta potential before and after removal of plasma proteins in Device 2.** (a) The liposomes are trapped in the 250 µm nanochannel length with a strong gradient ($ln(C_L/C_H) = -9.2$). (b) After the introduction of plasma (1:10 dilution) in the low salinity microchannel, and BSA (100 µM) at the high salinity microchannel, the proteins are removed by diffusion. The liposome distribution remains in the nanochannel and is fitted for the parameter ζ_{ch}. The Figure is supplementary to Figure 4(b, e) respectively.